| | |
|---|---|
| Title | Modern nuclear force predictions for the neutron-deuteron scattering lengths |
| Author(s) | Witala, H; Nogga, A; Kamada, Hiroyuki; Glockle, W; Golak, J; Skibinski, R |
| Issue Date | 2003-09 |
| URL | http://hdl.handle.net/10228/688 |
| Rights | Copyright © 2003 American Institute of Physics |

# Modern nuclear force predictions for the neutron-deuteron scattering lengths

H. Witała,[1,2] A. Nogga,[3] H. Kamada,[4] W. Glöckle,[5] J. Golak,[1] and R. Skibiński[1]
[1]*M. Smoluchowski Institute of Physics, Jagiellonian University, PL-30059 Kraków, Poland*
[2]*Department für Physik und Astronomie, Universität Basel, Basel, Switzerland*
[3]*Department of Physics, University of Arizona, Tucson, Arizona 85721, USA*
[4]*Department of Physics, Faculty of Engineering, Kyushu Institute of Technology, 1-1 Sensuicho, Tobata, Kitakyushu 804-8550, Japan*
[5]*Institut für Theoretische Physik II, Ruhr-Universität Bochum, D-44780 Bochum, Germany*
(Received 12 May 2003; published 5 September 2003)

The neutron-deuteron ($nd$) doublet ($^2a_{nd}$) and quartet ($^4a_{nd}$) scattering lengths were calculated based on the nucleon-nucleon ($NN$) interactions CD Bonn 2000, AV18, Nijm I, II, and 93 alone and in selected combinations with the Tucson-Melbourne (TM), a modified version thereof, TM99, and the Urbana IX three-nucleon ($3N$) forces. For each $NN$ and $3N$ force combination the $^3$H binding energy was also calculated. In case of TM99 and Urbana IX the 3NF parameters were adjusted to the $^3$H binding energy. In no case (using $np$-$nn$ forces) the experimental value of $^2a_{nd}$ was reached. We also studied the effect of the electromagnetic interactions in the form introduced in AV18. Switching them off for the various nuclear force models leads to shifts of up to $+0.04$ fm for $^2a_{nd}$, which is significant for present day standards. The electromagnetic effects also have a noticeable effect on $^4a_{nd}$, which is extremely stable under the exchange of the nuclear forces otherwise. Only if the electromagnetic interactions are included, the current nuclear forces describe the experimental value. As a consequence of the failure to reproduce $^2a_{nd}$ also the newly measured coherent $nd$ scattering length ($b_{nd}$) cannot be reproduced. The current nuclear force models predict $^3$H binding energies and the $^2a_{nd}$ values around an averaged straight line (Phillips line), but this correlation is broken visibly. This allows us to use $^2a_{nd}$ and the $^3$H binding energy as independent low-energy observables.

DOI: 10.1103/PhysRevC.68.034002 PACS number(s): 21.45.+v, 24.70.+s, 25.10.+s, 25.40.Lw

## I. INTRODUCTION

It has been observed a long time ago that the neutron-deuteron ($nd$) scattering length for total three-nucleon ($3N$) spin $S=1/2$ ($^2a_{nd}$) is correlated to the $^3$H binding energy ($E_{^3\mathrm{H}}$). This correlation is known as the Phillips line [1]. Indeed, calculations years later based on simplistic or more realistic nucleon-nucelon ($NN$) model forces (see Refs. [2–7]) yielded quite a few results for the $^3$H binding energy and the $^2a_{nd}$ scattering length, which lie on or rather close to a line in the two-dimensional plane spanned by $E_{^3\mathrm{H}}$ and $^2a_{nd}$. Also $3N$ forces of the $2\pi$-exchange type have been added. In Ref. [3] it was found that this line passes well through the experimental point.

In recent years chiral perturbation theory and effective theories have been applied to nuclear physics. In the pionless formulation [8–10], which is adequate for extreme low-energy phenomena, it has been shown that $^3$H can be energetically stabilized only if a $3N$ contact force is introduced (see, however, Refs. [11,12]). In the two lowest orders of that framework there is just one parameter connected to that $3N$ force. Thus both quantities, $E_{^3\mathrm{H}}$ and $^2a_{nd}$, depend on that one parameter and are therefore correlated though the line does not hit the experimental point. In higher orders additional parameters show up and the correlation is broken, which makes the two quantities independent. The same observation was made in an approach based on chiral perturbation theory [13] which includes explicitely the pion degrees of freedom. In the next-to-next-to-leading-order (NNLO), $3N$ forces occur the first time and they depend on two parameters. This makes $E_{^3\mathrm{H}}$ and $^2a_{nd}$ independent and the Phillips line correlation is broken. In fact, Ref. [13] uses the two experimental values to fix the two parameters of the $3N$ force [13]. Thus we find it interesting to ask, whether the conventional, high-precision $NN$ forces AV18 [14], CD Bonn 2000 [15], Nijm I, Nijm II, and Nijm 93 [16] alone or in combination with the two most popular $3N$ force models, Urbana IX [17] and TM99 [18,19] (an updated Tucson-Melbourne $2\pi$-exchange 3NF [20] modified in view of chiral symmetry) lead to a strict correlation between $E_{^3\mathrm{H}}$ and $^2a_{nd}$ or whether that Phillips line correlation is also absent. Further we ask whether the $NN$ and 3NF combinations adjusted to $E_{^3\mathrm{H}}$ (or may be only one of them) also describe $^2a_{nd}$. One more reason to confront $^2a_{nd}$ to state-of-the-art calculations is the recent appearance of a precision neutron interferometric measurement of the nd coherent scattering length ($b_{nd}$) [21].

The coherent scattering length $b_{nd}$ depends in addition to $^2a_{nd}$ also on the second $s$-wave scattering length for the state of total $3N$ spin $S=3/2$, $^4a_{nd}$. Because of the Pauli principle this quantity is supposed not to be sensitive to short range details of the nuclear forces. We also want to investigate that quantity in the light of modern nuclear forces.

Additionally, we would like to add two more investigations. Charge-symmetry breaking in the strong $NN$ forces is mostly pronounced in the states $^1S_0$, where the scattering lengths for the neutron-neutron ($nn$), $a_{nn}$, and proton-proton ($pp$), $a_{pp}$, systems are different. However, the value for $a_{nn}$ is still under debate [22,23]. Therefore we would like to present results where the $nn$ forces are replaced by the (strong) $pp$ forces. This will provide some insight into the magnitudes of the shifts in $^2a_{nd}$ caused by small changes in $a_{nn}$.

 

The other investigation is due to effects on the scattering lengths and $E_{^3\mathrm{H}}$ caused by electromagnetic interactions, mostly due to magnetic moment interactions (MMI's). MMI is a relativistic effect and including only that specific force is of course inconsistent, since other relativistic effects are not taken into account (see, for instance, Ref. [24] and references therein). But it is interesting to see this separate effect on ${}^2a_{nd}$ and ${}^4a_{nd}$ (the way they affect the binding energies of ${}^3$H and ${}^3$He is known and older results have been reconfirmed recently [25]). Here we hit some ''defects'' in current *NN* force models. The *NN* potentials CD Bonn 2000, Nijm I, II, and Nijm 93 are fitted directly to the *NN* data without taking electromagnetic interactions (EMI) into account (of course the point Coulomb force in case of the *pp* system has been included). Therefore the strong forces include the effects of the MMI's (and further electromagnetic corrections). To see the effects of the EMI's, we have to subtract them from the *NN* forces and compare to results without that subtraction. In case of AV18 the strong force plus separate EMI's have been fitted to the data. Thus the force free of EMI's is just the strong AV18 force alone. In this respect we have to define the strong force for AV18 differently than for the CD Bonn and Nijmegen interactions.

The paper is organized as follows. In Sec. II the theoretical formulation is briefly outlined. The results are given in Sec. III, and we end with a summary and an outlook in Section IV. More technical details are deferred to the Appendix.

## II. FORMULATION

We use the Faddeev scheme. Including a three-nucleon force a convenient basic formulation for one part $T$ of the $nd\to n+n+p$ breakup amplitude [26,27] is the integral equation

$$T=tP\phi+(1+tG_0)V_4^{(1)}(1+P)\phi+tPG_0T + (1+tG_0)V_4^{(1)}(1+P)G_0T. \tag{1}$$

The driving term contains the *NN* operator $t$, permutation operators $P$, the free $3N$ propagator $G_0$, and a part of the $3N$ force, $V_4^{(1)}$. Any $3N$ force can be split into three pieces, where for instance the first piece is symmetrical under exchange of particles 2 and 3, the second under 3-1 exchange, etc. Thus the quantity $V_4^{(1)}$ is the part symmetrical under 2-3 exchange like the operator $t$, which is supposed to act on the pair 2-3. Finally, $\phi$ is the initial channel state composed of the deuteron state and a momentum eigenstate of the projectile neutron. This integral equation can precisely be solved using partial wave decomposition in momentum space. For details see Refs. [26,28,29].

The operator $U$ for elastic scattering is given in terms of the amplitude $T$ by quadrature as follows:

$$U=PG_0^{-1}\phi+PT+V_4^{(1)}(1+P)\phi+V_4^{(1)}(1+P)G_0T. \tag{2}$$

We want to solve directly the integral equation (1) at the threshold of $nd$ scattering. This is for zero initial relative momentum $\vec{q}_0$ of the projectile and will directly lead to the scattering length. For the convenience of the reader we briefly sketch the necessary steps [30]. Our partial wave momentum space basis is denoted by $|pq\alpha\rangle$, where $p$ and $q$ are the magnitudes of standard Jacobi momenta and $\alpha$ is a string of angular momentum and isospin quantum numbers (see Refs. [26,28]). For the relative momentum $\vec{q}_0$ pointing in $z$ direction, we define the auxiliary amplitude

$$U_{\alpha,\lambda I}(p,q)=\sum_{m,m_d}\frac{\sqrt{4\pi\hat{\lambda}}}{\hat{j}}\left(\lambda 0\frac{1}{2}m\middle|Im\right)(j_dm_dIm|Jm_d+m) \times\langle pq\alpha|U|\phi\rangle \tag{3}$$

for the projectile nucleon with orbital angular momentum $\lambda$ ($\hat{\lambda}\equiv 2\lambda+1$) and total angular momentum $I$ combined with the deuteron total angular momentum $j_d=1$ to total $3N$ angular momentum $J$. From that amplitude one obtains the partial wave projected nd elastic scattering amplitude as

$$U^J_{\lambda' I',\lambda I}=\sum_{l'}\int p'^2dp'\,\phi_{l'}(p')U_{\alpha'_d,\lambda I}(p',q_0), \tag{4}$$

where $\phi_l(p)$ are the $s$- and $d$-wave components of the deuteron and $\alpha'_d$ contains the deuteron quantum numbers.

Finally, the projectile and the deuteron spins can be combined to the total spin $\Sigma$ and one obtains

$$U^J_{\lambda'\Sigma',\lambda\Sigma}=\sum_{I,I'}\sqrt{\hat{\Sigma}'\hat{I}'}(-)^{J-I'}\begin{Bmatrix}\lambda'\frac{1}{2}I'\\ j_dJ\Sigma'\end{Bmatrix}\sqrt{\hat{\Sigma}\hat{I}}(-)^{J-I} \times\begin{Bmatrix}\lambda\frac{1}{2}I\\ j_dJ\Sigma\end{Bmatrix}U^J_{\lambda' I',\lambda I}. \tag{5}$$

The $S$-matrix element is given in terms of $U^J_{\lambda'\Sigma',\lambda\Sigma}$ as

$$S^J_{\lambda'\Sigma',\lambda\Sigma}=\delta_{\lambda'\lambda}\delta_{\Sigma'\Sigma}-i\frac{4\pi}{3}mq_0(i)^{\lambda'-\lambda}U^J_{\lambda'\Sigma',\lambda\Sigma} \tag{6}$$

leading to the doublet and quartet scattering lengths for $q_0=0$,

$${}^2a_{nd}=\frac{2\pi}{3}mU^{1/2}_{0\,1/2,0\,1/2},$$

$${}^4a_{nd}=\frac{2\pi}{3}mU^{3/2}_{0\,3/2,0\,3/2}. \tag{7}$$

One also defines a coherent scattering length $b_{nd}$ as

$$b_{nd}=\frac{m_n+m_d}{m_d}\left[\left(\frac{1}{3}\right)^2a_{nd}+\left(\frac{2}{3}\right)^4a_{nd}\right]. \tag{8}$$

We defer the special form of the Faddeev integral equation (1) at $q_0=0$ to the Appendix. It is free of singularities

and, therefore, it can be as easily solved as a bound state problem. Also the explicit form of the elastic amplitude for $q_0=0$ is given there.

## III. RESULTS

We used the $NN$ forces CD Bonn 2000, AV18, Nijm I, II, and Nijm 93 alone or in various combinations with the three-nucleon forces Urbana IX (Urb IX), the older Tucson-Melbourne (TM) force, and the modified one (TM99). When we combine the Urbana IX 3NF with CD Bonn 2000, the strength of the repulsive part of this 3NF is reduced by multiplying it with the factor 0.812 in order to get the proper $E_{^3\mathrm{H}}$ (denoted by Urb in Table I).

Due to their non-negligible influence on the $nd$ scattering lengths, we took special care of the electromagnetic interactions. In the case of the AV18 potential it is clear how to separate the strong AV18 force from the electromagnetic parts because both are defined separately and added together for fitting the total force to the $NN$ data. In case of the $np$ system the EMI's are given in Eqs. (11), (12), and (15) of Ref. [14] and in Eq. (16) for the $nn$ system. [For the $np$ system we did not include the very small class IV charge asymmetric force $\propto \vec{L}\cdot 1/2(\vec{\sigma}_i-\vec{\sigma}_j)$. Also we neglected the energy dependence of the $\alpha'$.] This is different for the CD Bonn 2000 and Nijmegen potentials, which were fitted directly to the $NN$ data without adding to them other electromagnetic interactions than the point Coulomb force in the $pp$ system. Therefore in order to define the strong forces in the particular $NN$ system one needs to subtract the corresponding EMI, which we assume to be the same as in Ref. [14]. To be precise, for the $np$ system we subtract the $np$ EMI's as defined above from the $np$ CD Bonn and the Nijmegen forces. Similarly, for the $nn$ system, we subtract from CD Bonn the MMI as defined above. Since we also want to see the effect of replacing the strong $nn$ force by the strong $pp$ force we have to define the strong $pp$ CD Bonn and Nijmegen forces. To this aim we subtract from these forces the $pp$ EMI's as given in Eqs. (3)–(8) of Ref. [14] without the leading 1 in $F_c(r)$ from Eq. (10) of Ref. [14]. The leading 1 corresponds to the point Coulomb force, which was separately taken into account in the fits of these interactions to $pp$ data [31].

Before we report our results, we give some comments on our numerical accuracy. As usual, the partial wave decomposition is truncated at a certain total two-body angular momentum $j_{max}$. Figure 1 documents the convergence of $^2a_{nd}$ as a function of $j_{max}$ for CD Bonn. This shows that we reached an accuracy of about three digits, which also holds for the other $NN$ forces. Adding a three-nucleon force, we were limited to $j_{max}=5$ due to computer resources. Nevertheless, as Fig. 2 documents, the convergence reached for $^2a_{nd}$ is two digits. In case of $^4a_{nd}$ with $NN$ forces alone we reach four digits convergence and including a $3N$ force an accuracy close to that. This is documented in Fig. 3. The other numerical ingredients (discretization of the momenta) are safely under control. In all calculations we took into account charge dependence of the $NN$ forces using a simple "$\frac{2}{3}\,t_{pp(nn)}+\frac{1}{3}\,t_{np}$" rule to generate $t$ matrices in isospin $t=1$ $2N$ states [32]. The total isospin $T=3/2$ $3N$ states have been neglected [32]. We checked that their inclusion does not change $^4a_{nd}$ up to the fifth digit and the change of $^2a_{nd}$ is of the order of 0.1%. The triton binding energies have been obtained using $j_{max}=6$. They are accurate to 2 keV.

As an overview we show all our results for $^2a_{nd}$ and $E_{^3\mathrm{H}}$ in Fig. 4. We see a group of results based on $NN$ forces alone in the right half of the figure and another group close to the experimental area including $3N$ forces. We performed several investigations. First we take CD Bonn 2000 as it is (fitted to the $NN$ data) and use the $np$-$nn$ force combinations appropriate for the nd system. The EMI's in the $np$ and $nn$ systems are effectively included inside the strong forces. In case of AV18 we keep all electromagnetic corrections as in [14] except the energy dependence of $\alpha'$ [MMI's for the $nn$ system and the MMI's together with the one photon Coulomb term $V_{C_1}(np)$ for the $np$ system]. The corresponding predictions are shown as stars in Fig. 4. Since no $nn$ forces have been introduced for the Nijmegen interactions, we do not show similar results for these forces.

To see the effect of replacing the strong $nn$ forces by the strong $pp$ forces, we performed a second series of calculations, which can now include the Nijmegen interactions. The difference between $nn$ and $pp$ strong forces is mostly located in the different scattering lengths $a_{nn}$ and $a_{pp}$ (strong) and will therefore give some information how changes in $a_{nn}$ will show up in changes of $^2a_{nd}$. Since thereby we do not want to change the EMI's we keep in case of AV18 the $nn$ MMI. For the CD Bonn and the Nijmegen potentials the strong $pp$ potentials are defined as above and the $nn$ MMI (as for AV18) is added. The results are shown as five open circles in Fig. 4. A comparison for CD Bonn 2000 and AV18 shows that the $^3$H binding energy is decreased (as known before) and $a_{nd}$ increased when $nn$ forces are replaced by $pp$ forces. These two first investigations provide theoretical predictions for the $nd$ scattering lengths and triton binding energy including all electromagnetic interactions allowing for a comparison to the experiment. This will be done below.

Before coming to this comparison, we address the effects of the electromagnetic interactions themselves by switching them off while generating theoretical predictions. For the AV18 potential we just take the $np$-$nn$ and $np$-$pp$ strong force combinations alone, while in the cases of CD Bonn 2000, Nijm I, II, and 93 we use the corresponding strong forces obtained as described above. The resulting theoretical predictions are shown as pluses and squares in Fig. 4 for the $np$-$nn$ and $np$-$pp$ combinations, respectively. Again the binding energy is decreased and $a_{nd}$ increased when $nn$ forces are replaced by $pp$ ones. In contrast, the addition of EMI's decreases the binding energy and the scattering length.

We would like to summarize the individual results of these four investigations as a dashed ($np$-$nn$ with EMI's), a dotted ($np$-$pp$ with EMI's), a solid ($np$-$nn$), and a dashed-dotted ($np$-$pp$) straight line fitted in a $\chi^2$ sense. These lines are also shown in Fig. 4. They include the corresponding results with 3NF's (see below). We see a small shift of the

TABLE I. Doublet and quartet $nd$ scattering lengths $^2a$ and $^4a$ together with the coherent scattering length $b_{nd}$ for different $NN$ potentials and selected combinations with different 3NF's. All calculations have been done with $j_{max}=5$. The first and second rows within each group for the different potential or potential combinations show the values obtained with $np$-$pp$ strong potentials with and without EM interactions, respectively (see text for explanation). The third and fourth rows within the groups for the combinations based on AV18 or CD Bonn 2000 are the corresponding results, when the $pp$ strong $NN$ potential is replaced by the $nn$ one (keeping the $nn$ MMI in case that EMI are included). The last column shows our $^3$H binding energies. In the second column we also included the cutoff parameter $\Lambda$ for the TM and TM99 forces.

| Potential | $\lambda/m_\pi$ | $^2a$ (fm) | $^4a$ (fm) | $b_{nd}$ (fm) | $E_{^3\mathrm{H}}$ (MeV) |
|---|---|---|---|---|---|
| CD Bonn 2000 | | 0.976 | 6.347 | 6.837 | −7.946 |
| | | 1.011 | 6.324 | 6.833 | −7.989 |
| | | 0.925 | 6.347 | 6.812 | −8.005 |
| | | 0.943 | 6.324 | 6.798 | −8.048 |
| CD Bonn 2000+TM | 4.795 | 0.622 | 6.347 | 6.661 | −8.419 |
| | 4.795 | 0.661 | 6.324 | 6.657 | −8.463 |
| | 4.795 | 0.570 | 6.347 | 6.634 | −8.482 |
| | 4.795 | 0.590 | 6.324 | 6.622 | −8.528 |
| CD Bonn 2000+TM99 | 4.469 | 0.620 | 6.347 | 6.660 | −8.422 |
| | 4.469 | 0.658 | 6.324 | 6.656 | −8.466 |
| | 4.469 | 0.569 | 6.347 | 6.634 | −8.482 |
| | 4.469 | 0.589 | 6.324 | 6.622 | −8.527 |
| CD Bonn 2000+Urb | | 0.637 | 6.347 | 6.668 | −8.423 |
| | | 0.674 | 6.324 | 6.664 | −8.467 |
| | | 0.586 | 6.347 | 6.643 | −8.482 |
| | | 0.607 | 6.325 | 6.630 | −8.526 |
| AV18 | | 1.304 | 6.346 | 7.001 | −7.569 |
| | | 1.319 | 6.326 | 6.988 | −7.606 |
| | | 1.248 | 6.346 | 6.973 | −7.628 |
| | | 1.263 | 6.326 | 6.960 | −7.666 |
| AV18+TM | 5.215 | 0.614 | 6.346 | 6.656 | −8.478 |
| | 5.215 | 0.633 | 6.326 | 6.645 | −8.518 |
| | 5.215 | 0.556 | 6.346 | 6.627 | −8.545 |
| | 5.215 | 0.575 | 6.326 | 6.616 | −8.584 |
| AV18+TM99 | 4.764 | 0.645 | 6.346 | 6.671 | −8.417 |
| | 4.764 | 0.663 | 6.326 | 6.660 | −8.457 |
| | 4.764 | 0.587 | 6.346 | 6.643 | −8.482 |
| | 4.764 | 0.606 | 6.326 | 6.632 | −8.522 |
| AV18+UrbIX | | 0.636 | 6.347 | 6.667 | −8.418 |
| | | 0.654 | 6.326 | 6.656 | −8.458 |
| | | 0.578 | 6.347 | 6.638 | −8.484 |
| | | 0.597 | 6.326 | 6.628 | −8.523 |
| Nijm I | | 1.158 | 6.342 | 6.924 | −7.742 |
| | | 1.190 | 6.321 | 6.919 | −7.782 |
| Nijm I+TM | 5.120 | 0.601 | 6.342 | 6.646 | −8.493 |
| | 5.120 | 0.638 | 6.321 | 6.643 | −8.535 |
| Nijm I+TM99 | 4.690 | 0.594 | 6.342 | 6.642 | −8.485 |
| | 4.690 | 0.629 | 6.321 | 6.638 | −8.528 |
| Nijm II | | 1.231 | 6.345 | 6.964 | −7.663 |
| | | 1.259 | 6.325 | 6.957 | −7.700 |
| Nijm II+TM | 5.072 | 0.598 | 6.345 | 6.647 | −8.500 |
| | 5.072 | 0.630 | 6.325 | 6.643 | −8.540 |
| Nijm II+TM99 | 4.704 | 0.597 | 6.345 | 6.646 | −8.487 |
| | 4.704 | 0.627 | 6.325 | 6.642 | −8.527 |
| Nijm 93 | | 1.196 | 6.343 | 6.944 | −7.672 |
| | | 1.225 | 6.322 | 6.937 | −7.712 |
| Nijm 93+TM | 5.212 | 0.574 | 6.343 | 6.633 | −8.502 |
| | 5.212 | 0.608 | 6.322 | 6.629 | −8.543 |

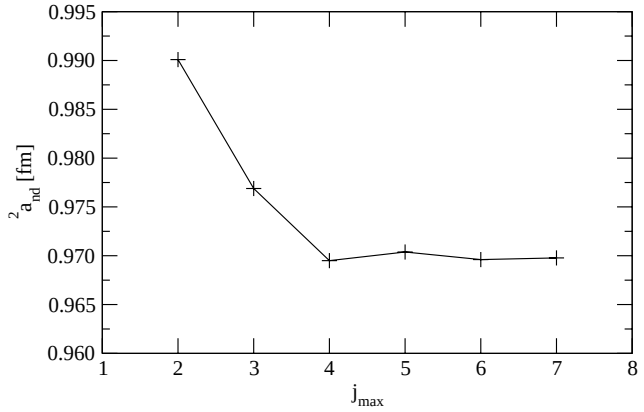


FIG. 1. The convergence of the doublet scattering length $^2a_{nd}$ as a function of the $2N$ total angular momentum $j_{max}$ for the CD Bonn potential.

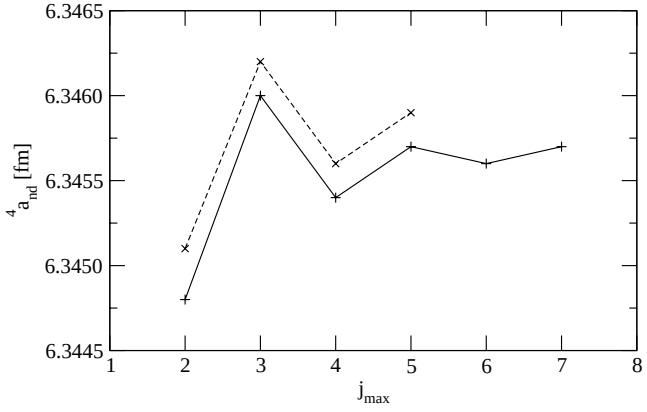


FIG. 3. The convergence of the quartet scattering length $^4a_{nd}$ as a function of $j_{max}$ for the CD Bonn potential (solid curve) and its combination with the TM 3NF (dashed curve).

lines under exchanges of $nn$ versus $pp$ forces, but a more significant shift if the electromagnetic forces are switched off. Though the two curves (dashed and dotted) for the cases when the electromagnetic forces are added come close to the experimental range spanned by the uncertainty in $^2a_{nd}$, they miss it clearly. If the electromagnetic forces are switched off the $np$-$nn$ (solid) and $np$-$pp$ (dashed-dotted) lines go through the experimental point well inside the $^2a_{nd}$ error bar. This should be considered as accidental.

Now we want to regard our results in more detail as displayed in Table I and in the inset of Fig. 4. The theory has to be finally compared to the experimental values, which are $^2a_{nd}=(0.65\pm0.04)$ fm [33], $^4a_{nd}=(6.35\pm0.02)$ fm [33], and $b_{nd}=(6.669\pm0.003)$ fm [21].

The results in Table I are grouped into $NN$ force predictions only and selected combinations with the $3N$ forces TM, TM99, and Urbana IX. For each potential or potential combination we show the results for the various scattering lengths and the $^3$H binding energies. These are given for the $np$-$pp$ $NN$ forces, with (without) EMI's in the first (second) row. For AV18 and CD Bonn 2000 we also show the results for $np$-$nn$ forces with (third row) and without (fourth row) electromagnetic interactions. Note that in case of the $np$-$nn$ forces including EMI's (as described above) the combinations with TM99 and Urbana IX are well fitted to the experimental value $-8.48$ MeV of the $^3$H binding energy. For Nijm I and II similarly accurate fits were performed based on the $np$-$pp$ forces. For the older TM $3N$ force we did not perform a precise (re)fit and the results are only included in view of investigating, whether a straight line correlation between $^2a_{nd}$ and $E_{^3\mathrm{H}}$ exists. A glance at Fig. 4 tells us that the individual results scatter around the four straight lines. Thus obviously no straight line correlation exists (this has been known before, though for some older calculations the numerical accuracy was maybe not sufficient to give a reliable judgement).

Let us now concentrate on the group of results with $3N$

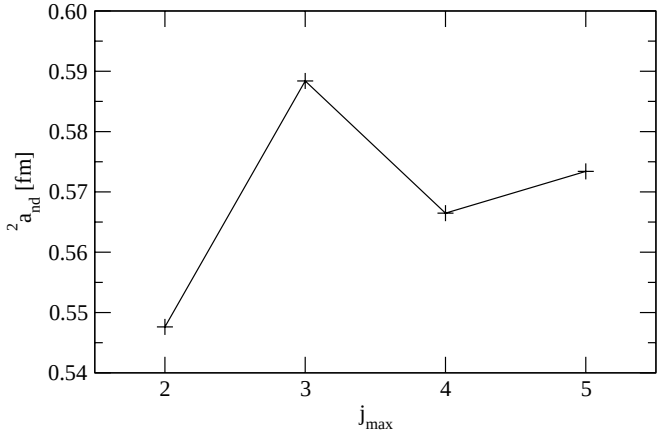


FIG. 2. The same as in Fig. 1, but for the CD Bonn potential combined with the TM 3NF.

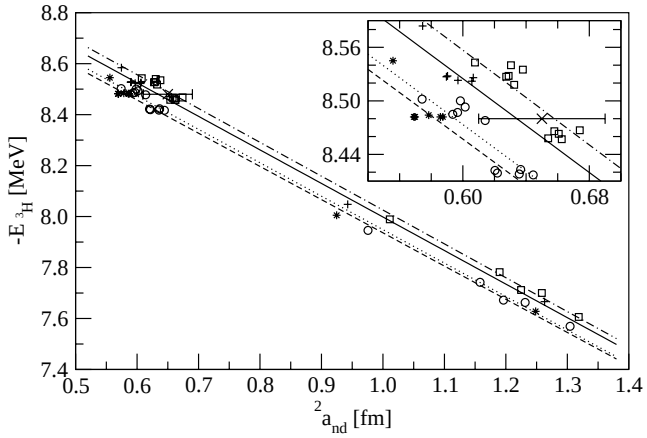


FIG. 4. The results for $^2a_{nd}$ and $E_{^3\mathrm{H}}$ from Table I: $np$-$nn$ forces alone (pluses), $np$-$pp$ forces alone (squares), and $np$-$nn$ and $np$-$pp$ forces plus electromagnetic interactions (stars and circles, respectively). The four straight lines (Phillips lines) are $\chi^2$ fits ($np$-$nn$, solid; $np$-$pp$, dashed-dotted; $np$-$nn$ with EMI's, dashed; $np$-$pp$ with EMI's, dotted). The lines with EMI's miss the experimental error bar for $^2a_{nd}$ [33]. The physically interesting domain around the experimental values is shown in the inset.

forces. These are displayed in the inset of Fig. 4. We see four results (stars) for the *np-nn* forces including TM99 or Urbana IX, where the binding energy has been exactly fitted but where the $^2a_{nd}$ value is too small. These are the results achieved under the supposedly most realistic assumptions of this paper. If one switches off the electromagnetic interaction (pluses) the binding energy increases and interestingly $^2a_{nd}$ moves to larger values. Regarding all results, the inclusion of the electromagnetic force in our studies shows that they cause shifts of up to about 40 keV less binding energy and of up to about 0.04 fm decrease in $^2a_{nd}$. In no case studied the experimental value of $^2a_{nd}$ is reproduced for *np-nn* or *np-pp* strong forces and *nn* EMI's combined with different 3NF's with the exception of *np-pp* AV18 combined with TM 3NF, for which the theoretical prediction lies at the lower limit of the error bar.

As one learned from the approach in chiral perturbation theory [13], where two parameters are needed to fix the short range $3N$ forces at NNLO and consequently two $3N$ observables to adjust them, one could foresee that the straight lines in Fig. 4 could only by accident pass through the experimental region. For the conventional forces used in this paper, one can think of additional $3N$ force diagrams (the most obvious one the $\pi$-$\rho$ exchange) where a sufficient number of parameters would be available to fit both, $E_{^3\mathrm{H}}$ and $^2a_{nd}$.

Going back to Table I we see that $^4a_{nd}$ sticks always close to the value 6.34 for the *np-pp* and *np-nn NN* force choices, without or with $3N$ forces and with EMI's included. This is well within the experimental $^4a_{nd}$ error bar. Interestingly, the electromagnetic interactions increase $^4a_{nd}$ in nearly all cases by about 0.02 and the pure strong force predictions lie always outside the experimental error bar.

Finally, one can confront theory to the very precisely known experimental value of the coherent scattering length $b_{nd}$ [21]. Clearly the supposedly most realistic dynamics (*nn-np NN* forces plus TM99 or Urbana IX 3NF's) misses that value. As can be seen from Table I, when electromagnetic interactions are included, the *np-pp* force combination reaches the experimental value in case of the AV18 and CD Bonn 2000 potentials combined with Urbana IX and AV18 with TM99. However, this agreement is accidental and caused by the corresponding decrease in $^3$H binding.

## IV. SUMMARY AND OUTLOOK

A recently performed precise neutron interferometric measurement of the *nd* coherent neutron scattering length [21] and a planned precision measurement of the doublet *nd* scattering length [34] stimulated us to investigate the theoretical predictions of that quantity for the high-precision *NN* forces CD Bonn 2000, AV18, Nijm I, II, and 93 in combination with currently popular $3N$ force models. These are the modified $2\pi$-exchange Tucson-Melbourne (TM99) and the Urbana IX $3N$ forces. We have chosen several *NN* and 3NF combinations, which are separately adjusted to the $^3$H binding energy. For *NN* forces alone with and without EMI's we recovered the approximate correlation between $E_{^3\mathrm{H}}$ and $^2a_{nd}$, but the scatter around a thought straight line (Phillips line) inside the band spanned by the four lines in Fig. 4 is quite strong. Adding $3N$ forces shifts the values into the neighborhood of the experimental range of $^2a_{nd}$, but misses the experimental value including its error bar in all cases, where electromagnetic forces are included. The inset of Fig. 4 clearly shows that for equal or nearly equal $^3$H binding energies $^2a_{nd}$ can vary significantly and vice versa.

Thus one has to conclude that $^2a_{nd}$ has to be considered as a low-energy observable, which is independent from the $^3$H binding energy. This observation has been found before in approaches based on pure effective field theory (pionless formulation) and on chiral perturbation theory (including pion degrees of freedom). Thus in future investigations, adjusting both observables, $E_{^3\mathrm{H}}$ and $^2a_{nd}$, for conventional nuclear forces will require more flexibility in the choice of $3N$ forces. Adding more mechanisms (on top of the $2\pi$ exchange) for $3N$ forces should be no obstacle. This is a step already performed in the effective theory approaches [8–10,13].

We also investigated the effects on $^2a_{nd}$ resulting from electromagnetic interactions given in Ref. [14]. The effects on $^2a_{nd}$ and even $^4a_{nd}$ are noticeable. For $^2a_{nd}$ including the electromagnetic interactions reduces its value by up to 0.04 fm. It is interesting to note that $^4a_{nd}$ is perfectly stable under all exchanges of nuclear forces studied in this paper but the electromagnetic interactions affect its value, though only in the third digit. However, only when EMI's are included the experimental value is reproduced.

The effects of adding the electromagnetic interactions on the $^3$H binding energy are well known and can reach shifts of up to 40 keV less binding energy.

Due to the failure to describe $^2a_{nd}$ also the recently measured coherent scattering length $b_{nd}$ cannot be reproduced theoretically. The good reproduction of $^4a_{nd}$ by all interactions and the small error bar of the coherent scattering length suggests that the value of the doublet *nd* scattering length might be somewhat smaller than the presently accepted experimental one, namely, around 0.63 fm. This strongly calls for a new, more precise measurement.

Since the scattering lengths are (extreme) low-energy observables, it appears that the mentioned effective theory approaches are the most adequate ones. Because these only use momenta below a certain cutoff, which is smaller than the nucleon mass, they also allow to incorporate relativistic effects in a well defined and convergent manner. Also $3N$ forces appear in these approaches in a well organized way, based a certain power counting scheme, and are consistent with the *NN* forces. In other words, one can take into account all these subtle effects, relativity, $3N$ forces, isospin breaking, in a well controlled and systematic manner. In conventional approaches on the other hand, which include a lot of phenomenological parametrizations and where no momentum cutoff is used, a reliable treatment of relativistic effects still poses a problem. Also the choices of $3N$ force mechanisms are quite unsettled.

Therefore, in conventional approaches reliable predictions for ${}^2a_{nd}$ will very likely remain a challenge for quite some time.

## ACKNOWLEDGMENTS

This work was supported by the Deutsche Forschungsgemeinschaft (J.G.,R.S.), by NFS Grant No. PHY0070858, by the Polish Committee for Scientific Research under Grant No. 2P03B00825, and by NATO Grant No. PST-.CLG.978943. R.S. acknowledges financial support of the Foundation for Polish Science. The authors would like to thank Dr. E. Epelbaum for very constructive discussions. The numerical calculations have been performed on the Cray T90, SV1, and T3E of the NIC in Jülich, Germany.

## APPENDIX

This appendix summarizes various expressions exactly at the $nd$ threshold $q_0=0$. The first part of the driving term in Eq. (1) turns out to be

$$\langle pq\alpha|tP|\phi\rangle=\delta_{\lambda_0,0}\sum_{l_{\alpha'}I_0}\left\langle pl_\alpha\left|t^\alpha\left(-\frac{3}{4m}q^2\right)\right|\frac{q}{2}l_{\alpha'}\right\rangle\varphi_{\alpha_0}(q)\times(1m_dI_0m_n|JM)\left(\lambda_00\frac{1}{2}m_n\middle|I_0m_n\right)\sqrt{\frac{\hat{\lambda}_0}{4\pi}}. \tag{A1}$$

The quantities with index 0 refer to the initial state.

The kernel applied on $T$ is given as

$$\langle pq\alpha|tG_0PT=\int q''^2dq''\int_{-1}^{+1}dx\,\frac{\sum_{l_{\alpha'}}\frac{m}{qq''}\frac{t^{l_\alpha,l_{\alpha'}}\left(p,\pi_1;-\frac{3}{4m}q^2\right)}{\pi_1^{l_{\alpha'}}}\sum_{\alpha''}\frac{G^-_{\bar{\alpha}\alpha''}(q,q'',x)}{\pi_2^{l_{\alpha''}}}\langle\pi_2q''\alpha''|T}{x_0-x} \tag{A2}$$

with

$$x_0\equiv\frac{-k_d^2-q''^2-q^2}{qq''} \tag{A3}$$

and $\bar{\alpha}$ contains the same quantum numbers as $\alpha$ with the exception of $l_\alpha$ replaced by $l_{\alpha'}$.

For our notation see Ref. [28]. The deuteron binding energy is written as $(-k_d^2/m)$. The remaining parts related to $V_4^{(1)}$ can be worked out correspondingly and can be found in Ref. [35]. Evaluating the elastic scattering amplitude one needs it at $q=q_0$ [see Eq. (4)]. Therefore the point $q=q_0=0$ was included. Then Eq. (A2) simplifies to

$$\langle pq=0\alpha|tG_0PT=2m\delta_{\lambda_{\alpha'},0}\int q''^2dq''\sum_{l_{\alpha'}}\frac{t^{l_\alpha,l_{\alpha'}}(p,q'';0)\sum_{\alpha''}2^{l_{\alpha''}}g^{0l_{\alpha'}0l_{\alpha''}0}_{\bar{\alpha}\alpha''}\left\langle\frac{1}{2}q''q''\alpha''\right|T}{-k_d^2-q''^2}. \tag{A4}$$

One ends up with the elastic scattering amplitude at threshold,

$$U^{J^\pi}_{\lambda'I',\lambda I}=-\frac{2k_d^2}{m}\delta_{\lambda,0}\delta_{\lambda',0}g^{00000}_{\alpha_{d'}\alpha_d}\sum_{l,l'}\left.\frac{\varphi_{l'}(p)}{p^{l'}}\right|_{p=0}\left.\frac{\varphi_l(p)}{p^l}\right|_{p=0}+\delta_{\lambda',0}\sum_{l',\alpha''}2^{l''+1}g^{0l'0l''0}_{\alpha_{d'}\alpha''}\int q''^2dq''\varphi_{l'}(q'')\left\langle\frac{1}{2}q''q''\alpha''\right|T$$
$$+\sum_{l'}\int p'^2dp'\varphi_{l'}(p')\{V_4^{(1)}(1+P)\phi+V_4^{(1)}(1+P)G_0T\}_{\alpha_{d'},\lambda I}(p',0). \tag{A5}$$

The geometrical coefficients $g^{kl_1l_2l_1'l_2'}_{\alpha\alpha'}$ arise from the permutation operator P and are given by Eq. (A19) in Ref. [28].

[1] A.C. Phillips, Nucl. Phys. **A107**, 209 (1968); Rep. Prog. Phys. **40**, 905 (1977).
[2] J.L. Friar, B.F. Gibson, and G.L. Payne, Phys. Rev. C **28**, 983 (1983).
[3] J.L. Friar, B.F. Gibson, G.L. Payne, and C.R. Chen, Phys. Rev. C **30**, 1121 (1984).
[4] J.L. Friar, Few-Body Syst., Suppl. **1**, 94 (1986).
[5] C.R. Chen, G.L. Payne, J.L. Friar, and B.F. Gibson, Phys. Rev. C **39**, 1261 (1989).
[6] A. Kievsky, M. Viviani, and S. Rosati, Nucl. Phys. **A577**, 511

(1994).
[7] A. Kievsky, Nucl. Phys. **A624**, 125 (1997).
[8] P.F. Bedaque, H.W. Hammer, and U. van Kolck, Nucl. Phys. **A646**, 444 (1998).
[9] P.F. Bedaque and U. van Kolck, Annu. Rev. Nucl. Part. Sci. **52**, 393 (2002).
[10] P.F. Bedaque, G. Rupak, H.W. Grieshammer, and H.W. Hammer, Nucl. Phys. **A714**, 589 (2003).
[11] B. Blankleider and J. Gegelia, nucl-th/0009007.
[12] B. Blankleider and J. Gegelia, in *Mesons and Light Nuclei*, edited by Jirí Adam, Petr Bydzovský, and Jirí Mares, AIP Conf. Proc. 603 (AIP, Melville, NY, 2001), p. 233.
[13] E. Epelbaum, A. Nogga, W. Glöckle, H. Kamada, U.G. Meissner, and H. Witala, Phys. Rev. C **66**, 064001 (2002).
[14] R.B. Wiringa, V.G.J. Stoks, and R. Schiavilla, Phys. Rev. C **51**, 38 (1995).
[15] R. Machleidt, Phys. Rev. C **63**, 024001 (2001).
[16] V.G.J. Stoks, R.A.M. Klomp, C.P.F. Terheggen, and J.J. de Swart, Phys. Rev. C **49**, 2950 (1994).
[17] B.S. Pudliner, V.R. Pandharipande, J. Carlson, Steven C. Pieper, and R.B. Wiringa, Phys. Rev. C **56**, 1720 (1997).
[18] J.L. Friar, D. Hüber, and U. van Kolck, Phys. Rev. C **59**, 53 (1999).
[19] S.A. Coon and H.K. Han, Few-Body Syst. **30**, 131 (2001).
[20] S.A. Coon *et al.*, Nucl. Phys. **A318**, 242 (1979); S.A. Coon and W. Glöckle, Phys. Rev. C **23**, 1790 (1981).
[21] T.C. Black (private communication).
[22] D.E. Gonzalez Trotter *et al.*, Phys. Rev. Lett. **83**, 3788 (1999).
[23] V. Huhn *et al.*, Phys. Rev. C **63**, 014003 (2000).
[24] H. Kamada, W. Glöckle, J. Golak, and Ch. Elster, Phys. Rev. C **66**, 044010 (2002).
[25] A. Nogga, A. Kievsky, H. Kamada, W. Glöckle, L.E. Marcucci, S. Rosati, and M. Viviani, Phys. Rev. C **67**, 034004 (2003).
[26] W. Glöckle, H. Witała, D. Hüber, H. Kamada, and J. Golak, Phys. Rep. **274**, 107 (1996).
[27] D. Hüber, H. Kamada, H. Witała, and W. Glöckle, Acta Phys. Pol. B **28**, 1677 (1997).
[28] W. Glöckle, *The Quantum Mechanical Few-Body Problem* (Springer-Verlag, Berlin, 1983).
[29] H. Witała, Th. Cornelius, and W. Glöckle, Few-Body Syst. **3**, 123 (1988).
[30] D. Hüber, W. Glöckle, J. Golak, H. Witała, H. Kamada, A. Kievsky, S. Rosati, and M. Viviani, Phys. Rev. C **51**, 1100 (1995).
[31] R. Machleidt, F. Sammarruca, and Y. Song, Phys. Rev. C **53**, R1483 (1996).
[32] H. Witała, W. Glöckle, and H. Kamada, Phys. Rev. C **43**, 1619 (1991).
[33] W. Dilg, L. Koester, and W. Nistler, Phys. Lett. **36B**, 208 (1971).
[34] O. Zimmer (private communication).
[35] D. Hüber, H. Witała, and W. Glöckle, Few-Body Syst. **14**, 171 (1993).